

A Model of Solar Dynamo with Alternative Conversion of Large-Scale Magnetic Field and Production of Sunspots

Biping Gong

Department of Physics, Huazhong University of Science and Technology, Wuhan 430074, China

Accepted, Received ;

ABSTRACT

Since the discovery of solar cycle related with magnetic field in 1908, deep seated oscillatory dynamo has been studied extensively. However, there are still open questions on the solar dynamo, e.g., asymmetric conversion between large-scale poloidal and toroidal field as well as physics underlying the butterfly pattern of sunspots. Here we report a new generation of large-scale magnetic field and process of energy release. The inductive action of fluid motions pervading the solar interior is represented by a RLC circuit in which the toroidal field built up through twisting of poloidal field, so called ω -effect, plays the role of a capacitor. Such a RLC circuit not only provides a self-sustained oscillatory system avoiding Cowling's antidynamo theorem, but also site of rapid magnetic reconnection which reproduces quadrupole magnetic field interpreting the behavior of sunspots and moving of foot-point in solar activities. Moreover, parameters of the circuit and the Sun are well consistent with the 22-year solar cycle.

1 INTRODUCTION

George Ellery Hale first linked magnetic fields and sunspots in 1908 (Hale 1908), who proposed that the sunspot cycle period is 22 years, covering two periods of increased and decreased sunspot numbers, accompanied by polar reversals of the solar magnetic dipole field. It indicated the existence of toroidal field, residing in solar interior as the source of sunspots

In 1919 Larmor proposed the inductive action of fluid motion as origin of such magnetic field, from which the twisting of large scale poloidal magnetic field by differential rotation in the solar interior is responsible for equatorial anti-symmetry of the solar internal toroidal field.

However, in 1933 Cowling demonstrated that even the most general purely axisymmetric flow could not sustain an axisymmetric magnetic field against Ohmic dissipation by themselves, which is known as Cowling's antidynamo theorem.

The theorem works e.g., in a Faraday's disk, consisting of an electromotive force (emf) of the disk, E , a power, $\mathbf{u} \times \mathbf{B} = u_\phi B_z$; and a term of energy dissipation, ηJ ,

$$\mathbf{E} = \eta \mathbf{J} - \mathbf{u} \times \mathbf{B} \quad (1)$$

Where J denotes current density, u_ϕ and B_z represents plasma velocity due to the rotation of the disk, and poloidal field respectively as shown in Fig.1. In fact, Eq.1 is equivalent to a RL circuit which cannot sustain by itself.

In 1950s Parker suggested that cyclonic twist could be introduced by Coriolis force which gives rise turbulent fluid elements in the solar convection zone, and provides a way of conversion from toroidal field to poloidal field (α effect). This is equivalent to an additional term to the right hand

side of Eq.1 which can make a self-sustained system and avoid Cowling's theorem. This idea inspired subsequent development of mean-field electrodynamic, which became the mainstream solar dynamo models.

However, there are still some problems in the mean-field electrodynamics. E.g., 1) internal differential rotation required by the mean-field models deviates from the result of helioseismology.

2) In the context of buoyancy, magnetic fields strong enough to produce sunspots could not be stored in the solar convection zone for sufficient lengths of time for adequate amplification.

3) α effect and magnetic diffusivity operating in the mean-field electrodynamics was also called into question by theoretical calculations and numerical simulations (Charbonneau 2010).

In this paper, an additional term denoting the toroidal magnetic field generated through stretching of poloidal field through differential rotation of near the solar photosphere is added to the RL circuit of Faraday disk, as shown in Eq.1. Then a self-excited RLC circuit is obtained, in which the toroidal field is equivalent to a capacitor originating in the ω effect.

The role of L , C in the RLC circuit, their derivation and relationship with solar parameters have been discussed in this paper. These issues have not been addressed concretely although RLC solar cycle model has been discussed before (Polygiannakis et al. 1996).

In the new model, the conversion between the polar and toroidal field is through the emf of the RLC circuit, which is symmetric and easy to keep equivalence time of conversion between them (Section 2).

With the ω effect which build up toroidal field through stretching of poloidal field via differential rotation of the Sun, the toroidal field of prior solar cycle and the current one of opposite polarity are concentrated at lower and lower latitude, so that a X-point configuration is formed. Such a configuration together with radial emf produced by the RLC circuit provide sites of rapid magnetic reconnection, in which magnetic field reproducing sunspots originates in Hall current rather than buoyancy of magnetic field (Section 3). How such a modified Faraday disk model confronts with Cowling's antidynamo theorem is addressed (Section 4). A number of questions concerning solar cycle can be explained under such a new dynamo model (Section 5).

Consequently, the generation of large-scale field, the site and configuration of energy release of magnetic field, and mechanism of reproducing sunspots of this paper all differ from previous ones.

2 THE TWISTED MAGNETIC FIELD AND THE RLC CIRCUIT

In the scenario of a Faraday disk, the first term at right hand side of Eq.1 corresponds to an emf, $E_r = u_\phi B_z$. Integrating this emf along the convection zone of the Sun is read,

$$\xi_r = \int_{r_2}^{r_1} E_r dr = \frac{\Omega}{2}(r_2^2 - r_1^2)B_z \quad (2)$$

where $r_1 = 0.95R_\odot$ and $r_2 = 0.74R_\odot$ (where R_\odot is the radius of the Sun).

The azimuth motion of plasma around the axis of the Faraday disk, u_ϕ , as shown in Fig.1, corresponds to an inductance of,

$$L \approx \frac{\mu}{2r_1} \pi(r_1^2 - r_2^2) = 5.2 \times 10^2 (H) \quad (3)$$

where $\mu = \mu_0$ is the permeability, and the area of the disk is of $S \approx \pi(r_1^2 - r_2^2) = 5.5 \times 10^{17} m^2$.

The left hand side of Eq.1 corresponds to an emf of,

$$\xi_P = -S \frac{\partial B_z}{\partial t} = -L \frac{\partial I}{\partial t} \quad (4)$$

where I is the current of the circuit.

The second term at right hand side of Eq.1 corresponds to energy dissipation of the disk, $\eta \int_{r_2}^{r_1} j dr = \eta \frac{aI}{\Sigma} = RI$, where Σ is the cross-section of the current in the disk and $a = r_1 - r_2$. With the three terms above, Eq.1 becomes,

$$\xi_r - L \frac{\partial I}{\partial t} - RI = 0 \quad (5)$$

Apparently, such a circuit cannot self-sustained.

In the case of the Sun, the twisted field magnetic field, B_ϕ also induces electromotive force in radial direction in the right hand side of Eq.1. Taking into account of it, $\mathbf{E}_R = \mathbf{u}' \times \mathbf{B}'$, the general Ohm's law becomes,

$$\mathbf{E} = \eta \mathbf{J} - \mathbf{u}' \times \mathbf{B}' - \mathbf{u} \times \mathbf{B} \quad (6)$$

As indicated by helioseismology (Thompson et al. 2003), different latitude corresponds to different rotation speed. E.g., at latitude of 60° the rotation speed at $0.95R_\odot$ is only 380nHz, which is much slower than that at the equator (470nHz). And at latitude 15° , 30° , and 45° at radius $0.95R_\odot$ the rotating speeds are between 380nHz and

470nHz. Considering polar field line, B_z , at radius $0.95R_\odot$ is frozen between latitude 60° and the equator, then the deviation in differential rotation speed between the two latitudes is of 100nHz(Thompson et al. 2003). In such a discrepancy, the field line is approximately wounded up for 3 times per year.

In contrast, by the helioseismology (Thompson et al. 2003), the rotation speed are of 470nHz and 460nHz at r_1 and r_2 respectively in the equatorial plane. In other words, differential rotation is much significant in latitude than that in radial, so that the differential rotation in radial (r_1 and r_2) is neglected, as shown in Eq.2, which is treated as having the same rotation velocity, Ω .

Lynden-Bell (1996) defined a pitch of between the poloidal and wound up toroidal field. The twisting field can be written as,

$$B_\phi = \kappa \int_0^t B_z dt \quad (7)$$

where $\kappa \equiv n/P_0$, with n the number of twisting and P_0 the time scale of twisting field lines. In the case of $P_0 \approx 1$ years, and $n = 3$, and with polar field of $B_z \approx 2$ G, the toroidal field B_ϕ can be magnified up to $B \approx 30$ G through winding of field line in 5 years. Apparently, the wound up toroidal field, B_ϕ , lags the polar field B_z . Hence, the general Ohm's law, Eq.6 can be written as,

$$E_P = \eta J - u_\phi B_z + u_z B_\phi \quad (8)$$

The polar flux of the Faraday disk varies with $SB_z = LI = LI_0 \sin \omega t$, so that $B_z \propto I$. In comparison, Eq.7 indicates $B_\phi \propto \int_0^t B_z dt \propto \int_0^t I dt \propto q$. Therefore, the role of B_ϕ in is equivalent to a capacitor in an RLC circuit,

$$\xi_R = \int_{r_2}^{r_1} E_R dr = \int_{r_2}^{r_1} u_z B_\phi dr = u_z B_\phi a = \frac{q}{C} \quad (9)$$

Time derivative of Eq.9 and using Eq.7 yields,

$$\frac{1}{C} \frac{dq}{dt} = \frac{1}{C} I = \kappa u_z B_z a = \kappa u_z \frac{\mu I a}{2r_1} \quad (10)$$

With $u_z \approx 25$ m/s, $\kappa \approx 3/P_0$, $\mu = \mu_0$, and $r_1 = 0.95R_\odot$, the equivalent capacity is read,

$$C = \frac{2r_1}{\mu \kappa u_z a} \approx 2.1 \times 10^{13} (F). \quad (11)$$

On the other hand, with a height of a cylinder of $\Delta h = R_\odot$, the capacity of a conventional capacitor, C' , can be calculated. Assuming $C = C'$ we have $\epsilon = 1.2 \times 10^3 (F/m)$ as shown in Table 1.

The time derivative of general Ohm's law of Eq.8 gives,

$$L \frac{d^2 I}{dt^2} + \frac{I}{C} + R \frac{dI}{dt} = \frac{\partial \xi_r}{\partial t} \quad (12)$$

With the values of L and C given by Eq.3 and Eq.10, the oscillation period of such a RLC circuit as given by Eq.12 is read,

$$P = 2\pi \sqrt{LC} = 2\pi \sqrt{5.2 \times 10^2 \times 2.1 \times 10^{13}} \approx 21 (year) \quad (13)$$

In other words, the RLC circuit with the capacitor and inductance derived from the parameters such as u_z , κ , S , r_1 , and μ , ξ automatically oscillates at a period of approximately 22-year.

The impedance of the resistor, R , the coil, L , and the

capacitor, C , in the circuit of Eq.12 are $Z_R = R$, $Z_L = i\omega L$, $Z_C = \frac{1}{i\omega C}$, respectively. The total impedance of such a RLC circuit is

$$Z = \sqrt{(\omega L - 1/\omega C)^2 + R^2} \quad (14)$$

The power of the circuit totally dissipated on the resistor requires that $Z = R$ be satisfied in Eq.14, which means $\omega L = 1/\omega C$. This is consistent with Eq.13.

The polar field B_z and the twisted field B_ϕ correspond to the first (L) and second term (C) of Eq.12 respectively, which can converse each other at period given by Eq.13. Therefore, in the new dynamo the equal time of conversion between the polar and twisted field is a natural result of the RLC circuit.

The closed lines of Fig.1A represent a unit of RLC circuit, infinite number of which form the equivalent circuit as shown in the middle of Fig.1. Such a RLC circuit can be described by Eq.12 with an intrinsic frequency of oscillation of $\omega_0 = 2\pi/\sqrt{LC}$ as shown in Eq.13.

At the right hand side of Eq.12 is a derivative of ξ_r given by Eq.2, which can be rewritten as

$$\frac{\partial \xi_r}{\partial t} = b \frac{\partial B_z}{\partial t} \quad (15)$$

where $b = \Omega(r_2^2 - r_1^2)/2$. Substitute $B_z \approx \mu I/2r_1$, and the current of the RLC circuit of $I = I_0 \sin \omega t$, into Eq.15, we get,

$$\frac{\partial \xi_r}{\partial t} = \frac{b\mu I_0 \cos \omega t}{2r_1}, \quad (16)$$

The oscillation of the RLC circuit of Eq.12 can be seen as a response of the circuit to the external “force”, $\partial \xi_r / \partial t$ of Eq.16,

$$I = \frac{h}{[(\omega_0^2 - \omega^2)^2 - 4\gamma^2 \omega^2]^{1/2}} \cos[\omega t + \alpha] \quad (17)$$

where $h = \omega b \mu I_0 / (2r_1)$, $\gamma = R/(2L)$, and $\beta = \alpha + \frac{\pi}{2} = \tan^{-1} \frac{\omega_0^2 - \omega^2}{2\gamma\omega}$.

As shown Fig.2, the phase discrepancy between the sin function of the polar field, and cos function denoting sunspot number is of $\delta = 9.7^\circ$, which requires the angle of β defined under Eq.17 to be $\beta = 99.7^\circ$.

To have such a β in the case of $|\omega - \omega_0|/\omega_0 \sim 10^{-1}$, demands

$$\tan^{-1} \left[\frac{-\omega_0}{10\gamma} \right] \approx 99.7^\circ \quad (18)$$

which requires, $\gamma \approx 1.5 \times 10^{-10}$. In such a case we have, $R = 2L\gamma \approx 1.5 \times 10^{-7} (\Omega)$ (so that $\sigma = 7 \times 10^6 S/m$).

Recall the flux of polar field varies with $SB_z = LI = LI_0 \sin \omega t$, the phase of which deviates from that of energy dissipation of $I^2 R \propto \cos^2[\omega t + 9.7^\circ]$ for approximately $\pi/2$.

In contrast, the change of B_ϕ lags about $\pi/2$ from the polar field due to the effect of twisting as shown in Eq.7, so that the twisted field varies with $B_\phi \propto \cos \omega t$. Therefore, the energy of the twisted field varies with $\frac{B_\phi^2}{2\mu} V \propto \cos^2 \omega t$; which is approximately in phase with $I^2 R \propto \cos^2(\omega t + 9.7^\circ)$.

The energy stored in the twisted field, $\frac{B_\phi^2}{2\mu} V$ is difficult to estimate due to the uncertainty in the involved volume V . Alternatively, it can be estimated by the equivalent current in the term, $B_\phi \approx \mu I_z / (2\pi r_1)$. With $B_\phi \approx 1 \times 10^{-3} T$, we have $I_z \approx 3 \times 10^{12} A$, corresponding to a power of $I_z^2 R \approx$

$1.4 \times 10^{18} W$, so that it can dissipate the energy of $1 \times 10^{25} J$ in every 5 months.

Then in a half solar cycle of 11 years, the energy release from such a RLC circuit is of $\sim 10^{26} J$. Whereas, such an amount of energy is not released evenly in 11 years, instead the majority energy is released in a few years during the peak of the toroidal field through magnetic reconnection.

3 MAGNETIC RECONNECTION

As shown in Fig.2, the poloidal field e.g., the south field was at a minimum amplitude in around 1980 (solar cycle $n = 21$), then it increased with time and peaked at 1985-1987 (with $p_n^- \approx \max$). Later it reached the minimum again in around 1990.

The twisting of the south field of solar cycle 21 actually started at around 1980; and peaked in 1990 ($T_n^- \approx \max$), as shown in blue curve of Fig.2. The phase of the toroidal field lags the poloidal field for approximately one fourth solar cycle ($\pi/2$), which is expected by the RLC circuit as discussed in Section 2.

The peak of toroidal field, $T_n^- \approx \max$ in 1990 (red in Fig.1B) and the new toroidal field of next solar cycle 22 with opposite polarity, T_{n+1}^+ , (blue in Fig.1B) become closer and closer with stretching of field lines through differential rotation, which provide site of magnetic reconnection responsible for solar activity and peak of sunspot in around 1990, as shown in Fig.2.

In fact, as soon as T_n^- first emerged in around 1980, it formed a site of magnetic reconnection with toroidal field of prior solar cycle, T_{n-1}^+ , which was responsible for energy release and the peak of sunspots in around 1980.

Therefore, in every solar cycle, the maximum energy release is at the maximum B_ϕ corresponding to a phase of $\cos \omega t = 1$ (recall $B_\phi \propto \cos \omega t$). E.g., for toroidal field, T_n^- , the first maximum energy release occurred when T_n^- was as new toroidal field interacting with prior one, T_{n-1}^+ , and the second maximum of energy release happened when T_n^- as a old field interacting with the toroidal field of next solar cycle, T_{n+1}^+ . As shown in Fig.1, the toroidal field, T_{n-1}^+ being twisted for longer time is stronger in strength of magnetic field but weaker in flux than that of T_n^- .

The large-scale toroidal field, T_{n-1}^+ of prior solar cycle and the current one, T_n^- , form X-point configuration, Fig.1 and Fig.3a, which provide sites for magnetic reconnection. Can such reconnection explain the evolution of sunspots and be rapid enough to account for the fast release of stored magnetic energy?

In the reconnection of X-point configuration, magnetic field lines are frozen into the charged particles, both ions and electrons, whose motion are determined by $\mathbf{E} \times \mathbf{B}$, where \mathbf{B} is B_n and B_{n-1} and $E = J_r/\sigma$ as shown in Fig.3abd. Such a drift of plasma (Hall current), as shown in red lines of Fig.3bd, form “magnetic nozzle”.

To explain process of short timescales, Drake et al. (1997); Shay et al. (1999) has suggested that the energy release is instead mediated by electrons in waves called “whistlers”, moving much faster for a given perturbation of the magnetic field with their smaller mass. And as the “nozzle” becomes narrower, both the whistler velocity and associated plasma velocity increase.

Such a fast reconnection mediated by whistler waves is supported by the finding of quadrupole structure in the reconnection of magnetosphere (Deng & Matsumoto 2001).

Hall effect in reconnection and the generation of magnetic field of quadrupole pattern is also discussed (Zweibel & Yamada 2009).

The current, J_r , in the center of Fig.3bd (perpendicular to the plane) is driven by the radial emf, $E'_r = E_R - E_r$. Such an out-plane emf and the in plane magnetic field, T_{n-1} and T_n , together drive the plasma motion (Hall current) as shown in red arrows in Fig.3bd. Such an in-plane Hall current results in quadrupole pattern of magnetic field in Fig.3bd in photosphere of the Sun.

As T_{n-1} being twisted for longer time is stronger in strength of magnetic field than that of T_n , the quadrupole pattern of magnetic field has stronger dipole field near the field line T_{n-1} compared with that of T_n , as shown in Fig.3bd.

In such a case, a reversal of polarity of toroidal field corresponds to the reversal of the radial emf as shown in Eq.8. Accordingly, the polarity of Fig.3b and Fig.3d change in the first half and second half of a solar cycle respectively, which explains the reversal of polarity in the sunspots in each solar cycle, as shown in <http://solarscience.msfc.nasa.gov/images/magbfly.jpg>.

The large sunspot pairs, so called bipolar magnetic regions appear tilt with respect to the E-W direction, in which the leading sunspot, relative to the solar rotation, is located at a lower latitude than the trailing sunspot, the pattern of which is known as Joy's law. This can be explained by the X-point configuration of twisted field which moves closer and closer to the equator in the twisting, as shown in Fig.1 and Fig.3a.

Therefore, both the change of polarity and configuration of sunspots can be interpreted by the quadrupole structure in the reconnection of magnetosphere (Deng & Matsumoto 2001), which is located between the prior and current toroidal field. The observation of flare ribbons favors reconnection with preexisting field below the corona (Philip et al. 2017), which can be seen as reconnection of such X-points above such sunspots. Apparently, with the twisting of the prior and current cycle of field lines, the location of X-points varies so that the foot-point of such reconnection also moves.

With a velocity of plasma of $\sim 10m/s$, a length scale of $\sim 10Mm$ and the magnetic diffusivity of Table 1, magnetic Reynolds number is $R_m = vL/\eta \sim 10^9$. Such an extremely large magnetic Reynolds number in this turbulent environment resulting in the efficient generation of magnetic fields on extremely small scales (Jones et al. 2010), which explains activities, e.g., nano-flares to coronal mass ejections.

4 MODIFIED FARADAY DISK VS COWLING'S LAW

The induction equation with constant conductivity is read,

$$\frac{\partial \mathbf{B}}{\partial t} = \nabla \times (\mathbf{u} \times \mathbf{B}) + \eta \nabla^2 \mathbf{B} \quad (19)$$

In the case of axisymmetric magnetic field and flow, a simpler decomposition is

$$\mathbf{B} = B_\phi \hat{\phi} + \mathbf{B}_z, \mathbf{u} = s\Omega \hat{\phi} + \mathbf{u}_z \quad (20)$$

where $s = r \sin \theta$. The induction equation becomes (Jones et al. 2010),

$$\frac{\partial \mathbf{B}}{\partial t} + s(\mathbf{u}_z \cdot \nabla) \left(\frac{B}{s} \right) = \eta (\nabla^2 - \frac{1}{s^2}) B + s \mathbf{B}_z \cdot \nabla \Omega \quad (21)$$

This equation reveals some important aspects of the dynamo process. The advection term, $(\mathbf{u}_z \cdot \nabla)$, and the diffusion term, $(\nabla^2 - \frac{1}{s^2})$, cannot create magnetic field. Toroidal field can be generated from poloidal field via the term, $s \mathbf{B}_z \cdot \nabla \Omega$. In the case of the sun gradients of angular velocity are both along radial and latitude with the latter much stronger than that if the former (Thompson et al. 2003), poloidal field is thus stretched out by differential rotation of the latitude (as mentioned in Section 2) to generate toroidal field.

However, the poloidal field of Eq.21 has no source term, so it will just decay unless a mechanism can be found to sustain it (Jones et al. 2010). This is the argument of Cowling's antidynamo theorem.

In comparison, Eq.8 represent induction on a modified Faraday disk, in which the term denoting stretched field lines by differential rotation is added to the last term at right hand side of Eq.8 (the usual Faraday disk don't have such a term). In such a case B_ϕ is lagged for $\pi/2$ with respect to B_z due to stretching of field lines through differential rotation.

Consequently, there is no B_ϕ component that is in phase with component B_z in Eq.8, so that the left hand side of Eq.8 corresponds to $\partial B/\partial t = \partial B_z/\partial t$, rather than two components in the first term at left hand side of Eq.21.

Most importantly, there is a term extracting rotation energy of the Sun to generate a radial emf as shown in Eq.2, which is also displayed the second term at right hand side of Eq.8. It is this term that works as source to the poloidal field, and then converse to toroidal field which makes a self-sustained oscillation and thus avoided Cowling's antidynamo theorem. In other words, Eq.21 is not self-sustain because it short of such a source term.

5 DISCUSSION

As discussed above, the dynamo model base on modified Faraday disk not only avoids Cowling's antidynamo theorem, so that an oscillation of 22 years well account for solar cycle; but also provides site and current to trigger rapid magnetic reconnection with polarity change consisting with the behavior of sunspots.

Notice that magnetic diffusivity of Table 1 is obtained under Eq.18, which is consistent with the oscillation period of Eq.13 calculated by parameters u_z , κ , S , r_1 , and μ , ξ of the Sun.

As discussed above, buoyancy of field lines is not necessary in the generation of sunspots, while considering buoyancy of the head of the twisted B_ϕ , as shown Fig.3a, and with current corresponding to purple curve of Fig.1a reconnection resembling the prominence is expected. Moreover, the polarity of such a morphology changes with the polarity of B_ϕ in each solar cycle, which can be tested by observations.

As shown in Fig.1 and Fig.3a, new model implies that the toroidal field at the northern and southern hemisphere of the Sun is antisymmetric, which is consistent with observations.

Table 1. Estimated parameters of the RLC circuit

$\epsilon(F/m)$	$\mu(N/A^2)$	$\sigma(S/m)$	$\eta(m^2/s)$	$C(F)$	$L(H)$
1×10^3	$4\pi 10^{-7}$	7×10^6	0.1	2×10^{13}	5×10^2

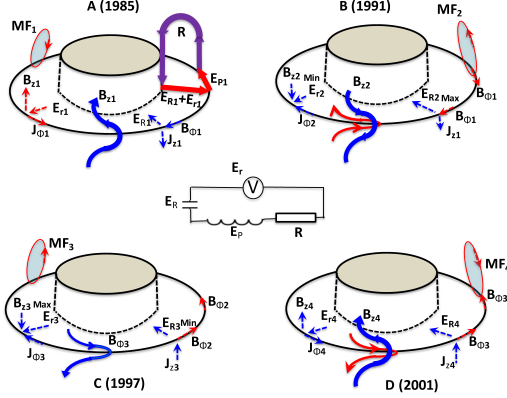


Figure 1. A schematic show of the RLC circuit in the Faraday disk. The out and inner circles denote the radii $0.95R_{\odot}$ and $0.74R_{\odot}$ respectively in the equatorial plane of the Sun. The ellipses in the four panels (A,B,C,D) represent the meridional flows (e.g., MF1 and MF2). The red and blue curves denote toroidal field produced by the prior solar cycle and current cycle respectively. The closed lines in panel A form a unit RLC circuit, with E_r and E_R in the radial plane of the disc, E_P along the disk ring, and the rest of the lines denote the resistance of the circuit. The sum of infinite number of such circuits around the axis of the disk for 360 degrees gives the equivalent circuit in the middle.

The sum of toroidal field at different latitudes corresponds to an eddy current as shown in Fig.1a-d, which explains the meridional circulation observed. Moreover, the meridional circulation of Fig.1a-d are affected by the change of polarity of the toroidal field in each solar cycle. However this don't mean that meridional circulation change from poleward to equator with the change of polarity of toroidal field. because the eddy current can change sign by switch to positive or negative charge under the same velocity of meridional flow. This can be tested by further observation.

REFERENCES

Hale, G.E., 1908, ApJ, 28, 315

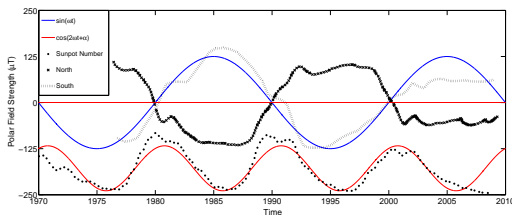


Figure 2. Observed (black) and simulated number of sunspots and the polar field (red and blue).

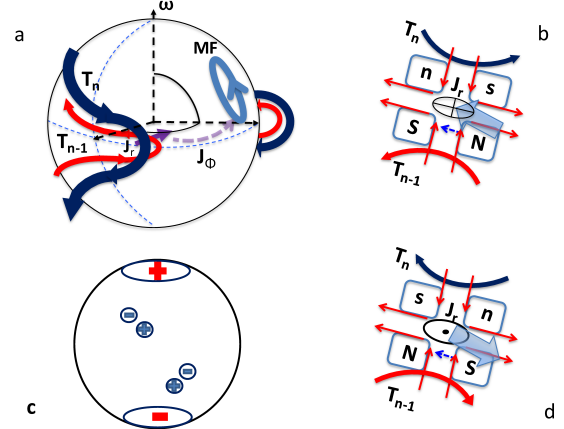


Figure 3. A schematic show of twisted field and resultant reconnection configurations. Panel a exhibits the configuration of toroidal field of prior and current solar cycle, which provides site of magnetic reconnection. Panel b displays reconnection between T_{n-1} and T_n with current, J_r , driven by the radial emf of the RLC circuit. Plasma motion (Hall current) as shown in red arrows results in quadrupole pattern of magnetic field. Panel d is the same as panel b but with opposite polarity. Panel c shows observational polarity of polar field and polarity of sunspots.

- Charbonneau, P., 2010, Living Rev. Solar Phys., 7, 3.
 Thompson, Michael J., Christensen-Dalsgaard, Jorgen, Miesch, Mark S. & Toomre, Juri, 2003, Annu. Rev. Astron. Astrophys, 41, 599-643
 Lynden-Bell, D., 1996, MNRAS, 279, 389-401
 Drake, J. F., Biskamp, D. & Zeiler, A., 1997, Geophys. Res. Lett. 24, 2921-2924.
 Shay, M. A., Drake, J. F., Rogers, B. N., & Denton, R. E., 1999, Geophys. Res. Lett. 26, 2163-2166.
 Deng, X.H. & Matsumoto, H., 2001, Nature, 410, 29, 557-560
 G. Zweibel & Masaaki Yamada, 2009, Rev. Astron. Astrophys., 47, 291-332.
 Judge, Philip G., Paraschiv, Alin, Lacatus, Daniela, Donea, Alina, & Lindsey, Charlie, 2017, The Astrophysical Journal, 838, 138.
 Chris A. Jones, Michael J. Thompson, & Steven M. Tobias, 2010, Sci Rev, 152: 591-616
 Polygiannakis, J. M., Moussas, X., & Sonett, C. P., 1996, Solar Physics, 163, 193-203.